The influence of the iron based nanoparticles density in growth of carbon nanotubes by C-LCVD method

I. P. MORJAN[a,b], A. BADOI[a], C. CEAUS[c]
[a]*National Institute for Lasers, Plasma and Radiation Physics, 409 Atomistilor St., P.O. Box MG-36, R-077125 Bucharest, Romania*
[b]*IMT-Bucharest, 126A, Erou Iancu Nicolae street, 077190, PO-BOX 38-160, 023573, Bucharest, Romania*
[c]*Univ Bucharest, Fac Phys, 3NANO-SAE Res Ctr, R-077125 Bucharest, Romania*

The synthesis of carbon nanotubes (CNTs) by catalytic laser induced chemical vapour deposition (C-LCVD) was investigated. The catalysts used in this study are Fe_2O_3 nanoparticles with a mean particle diameter of about 5 nm. Two catalyst suspensions were employed for the sake of comparison: one concentrated (20 g/l) and another one 10x diluted. The nanotubes were catalytically grown directly on a Si/SiO_2 substrate from C_2H_2/NH_3 gaseous precursors. Structural characterization of the samples by SEM, TEM and Raman spectroscopy was performed.

(Received March 18, 2013; accepted March 13, 2014)

Keywords: Carbon nanotubes, Iron based nano-catalyst, Catalytic Laser induced Chemical Vapour Deposition

1. Introduction

During the past decade carbon nanotubes (CNTs) have been extensively studied due to their outstanding mechanical, optical, thermal and electronic properties. With a broad range of potential applications including nanoelectronics, composites, chemical sensors, biosensors, microscopy, nanoelectromechanical systems, and many more, the scientific community is more motivated than ever to move beyond basic properties and explore the real issues associated with carbon nanotube-based applications [1].

Various production methods have been used to synthesize carbon nanotubes (CNTs). These methods can be broadly divided into chemical (e.g. chemical vapour deposition (CVD) [2] and aerosol synthesis [3]) and physical (e.g. arc discharge [4] and laser ablation [5]) according to the method applied to release carbon atoms from carbon-containing precursor. In CVD methods, the decomposition of the carbon precursor and CNT formation take place on the surface of previously made catalyst particles that are supported on a surface. In aerosol synthesis the catalyst particles are formed in situ during the CNT synthesis and the whole process takes place in the gas phase [6].

It has been widely accepted that the catalysts play a determinative role in tailoring the CNT structures and morphology as they are the active sites for CNT growth [7-9]. Following this line of interest, this work deepens the study of the catalysts, by investigating the role of the catalyst density in nanotubes growth and morphology. Much more, if the aggregation of catalyst particles is precisely controlled, one should be able to grow CNT arrays with desirable structural properties.

The laser induced chemical vapour deposition (LCVD) technique proposed in this study has several prominent advantages including: (i) high deposition rates, which is favourable for scale-up production of carbon nanotubes; (ii) minimum substrate and grown nanotubes damage, due to highly localized heating and excellent spatial resolution and process control; (iii) the capability to make carbon nanotubes networks and patterns by selected area deposition and laser direct writing techniques.

2. Experimental

The catalytic-LCVD (C-LCVD) synthesis of CNTs comprises two steps: (a) the preparation of the substrate by deposition, followed by pre-treatment of the catalyst nanomaterial and (b) the actual growth of nanotubes by C-LCVD. The catalysts used in this study are Fe_2O_3 nanoparticles with a mean particle diameter of about 5 nm obtained by the CW CO_2 laser pyrolysis [10].

In the first step, a concentrated catalyst suspension (CCS) (20 g/l) was prepared by stabilization with oleic acid and suspension in toluene of these nanoparticles**.** A diluted in toluene catalyst suspension (DCS) (10x dilution) will be employed for the sake of comparison. The seeding of the silicon substrate was realized by applying a drop of

the as-synthesized Fe_2O_3 catalyst suspension on the Si wafer. The C-LCVD system used for the carbon nanotubes growth was presented in detail elsewhere [11]. All experiments were performed by focussing the laser spot to 5 mm. The CO_2 laser (Coherent-Diamond E-400 OEM Laser System, $\lambda = 10.6$ μm) is used to heat the substrate by orthogonally intersecting both the reactant gas flow and substrate. An argon (Ar) flow is washing the entrance window. In order to reduce the oxidized surface of the Fe based nanoparticles, a pre-treatment procedure was applied to the catalyst nanoparticles: they were flushed during 1 minute under 450 mbar and 55 W laser power with a mixture of ammonia (NH_3) and Ar gases, using flow rates of 180 sccm and 1000 sccm.

In the second step of the C-LCVD synthesis, mixtures of acetylene (as carbon donor) and ammonia (as an energy transfer agent) were employed. The experimental parameters for the growth of CNTs by the catalytic LCVD are presented in Table 1. During all experiments the laser entrance window was flushed with 1000 sccm Ar, the total pressure in the reactor was held at 450 mbar and the irradiation time of the pre-deposited catalyst was 2 min.

Tabel 1. Experimental parameters for carbon nanotubes synthesis.

Using concentrated catalyst suspension (CCS)				**Using diluted catalyst suspension (DCS)**			
Set	**Sample**	**Gases: C_2H_2/NH_3 (sccm)**	**P_L (W)**	**Set**	**Sample**	**Gases: C_2H_2/NH_3 (sccm)**	**P_L (W)**
I	16S	30/90	50	**IV**	47S	30/90	50
	17S	30/90	55		48S	30/90	55
	24S	30/90	60		49S	30/90	60
II	26S	30/180	55	**V**	50S	30/180	55
	27S	30/180	60		51S	30/180	60
	28S	30/180	65		52S	30/180	65
III	31S	30/270	65	**VI**	53S	30/270	65
	44S	30/270	70		54S	30/270	70
	46S	30/270	75		55S	30/270	75

After synthesis, the CNTs were characterized by different analytical techniques including scanning electron microscopy (SEM) (using an InspectTM S50 apparatus), transmission electron microscopy (TEM) (TECNAI F30 G2 S-TWIN microscope operated at 300 kV) and Raman spectroscopy (using a Jasco NRS-3100 Laser Raman Spectrophotometer, λ=532 nm).

3. Results

In this paper, carbon nanotubes obtained from concentrated and diluted Fe_2O_3 nano-catalyst solutions are compared by studying their properties, at three reactants volumetric ratios, namely NH_3/C_2H_2 = 3/1, 6/1 and 9/1.

Raman spectroscopy, a technique which observes the energies of vibrational transitions in molecules, is a useful tool for studying carbon nanotubes. This technique yield information about the purity, defects and tube alignment, and offers the possibility to detect the presence of MWCNTs relatively to other carbon structures. The Raman spectra of the samples are displayed in Fig. 1.

Two main bands may be observed: the graphitic band (G-band, around 1580 cm^{-1}) and the disordered band (D-band, around 1350 cm^{-1}). The D-band originates from the atomic displacement and the disorder induced features caused by lattice defects, distortion or by the finite particle sizes, while the G-band represents the tangential mode vibrations of carbon atoms in graphene sheets, and its presence is associated with the formation of well-graphitized carbon nanotubes. The G′ band is attributed to a two-phonon second-order scattering process and is indicative of a long-range order in the sample [12].

In Fig. 2, the I_D/I_G and $I_{G'}/I_G$ ratio at different the laser powers and C_2H_2/NH_3 ratios are displayed. The intensity ratio between the D and G bands (I_D/I_G) gives information on the graphitic order of the synthesized carbon material: the lower the I_D/I_G, the better the structural order [13]. DiLeo et al propose that in multiwall CNTs disorder or defects will reduce this double resonance process decreasing the G' peak intensity providing a more accurate indication of CNT quality from the $I_{G'}/I_G$ ratio [14].

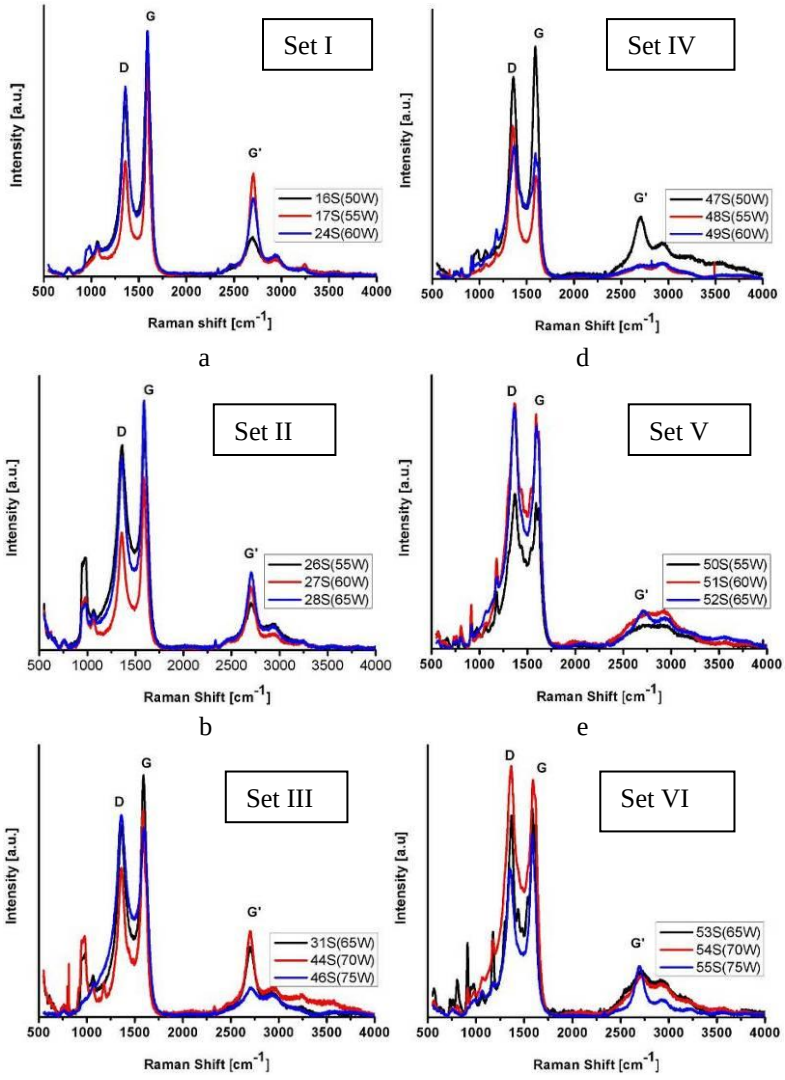

Fig. 1. Raman spectra of CNTs by using different catalyst suspensions: a, b, c –concentrated; d, e, f – diluted, for different laser powers and C_2H_2/NH_3 ratios (according to Table 1).

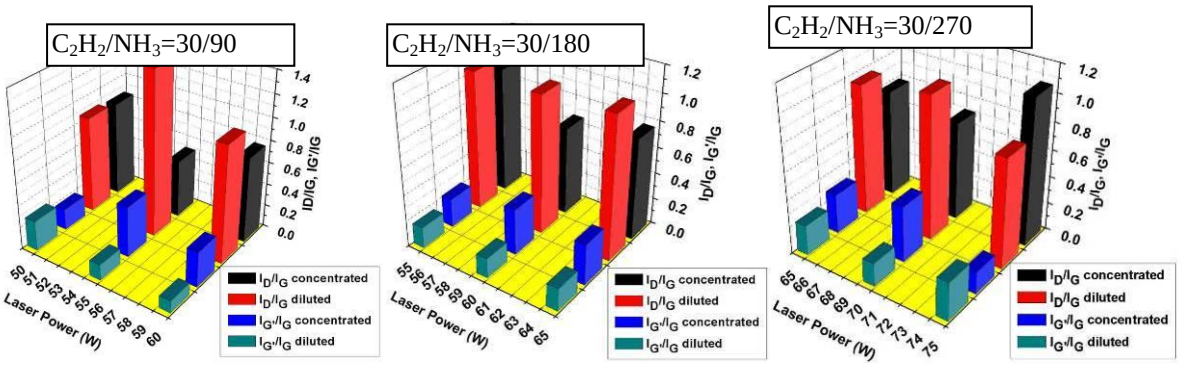

Fig. 2. Comparative histograms of calculated ID/IG and IG'/IG ratios from Raman spectra of the samples: (a) Set I and Set IV; (b) Set II and Set V; (c) Set III and Set VI.

The carbon structures obtained from CCS at medium C_2H_2/NH_3 ratio (C_2H_2/NH_3 = 30/180 (see Fig. 2b) show a good crystallinity (I_D/I_G<1), while those from DCS has a higher degree of disorder (I_D/I_G>1). By using CCS, at P_L= 60 W, sample 27S presents the lowest disorder degree from the Set II and V (I_D/I_G=0.67 and $I_{G'}/I_G$=0.35).

Fig. 2c shows the characteristics extracted from the Raman spectra of the samples obtained at the lowest C_2H_2/NH_3 ratio (C_2H_2/NH_3 =30/270). Sample 44S, obtained at 70 W laser power, has the best quality from the samples obtained by using CCS (I_D/I_G =0.72, $I_{G'}/I_G$ =0.41). Otherwise, from DCS seeded samples, the sample whose quality is the closest to the 44S is that synthesized at P_L=75 W (sample 55S, I_D/I_G =0.8 and $I_{G'}/I_G$ =0.28).

Scanning electron microscopy (SEM) is used subsequently to identify the presence and location of the nanostructures relatively to the Si/SiO_2 substrate.

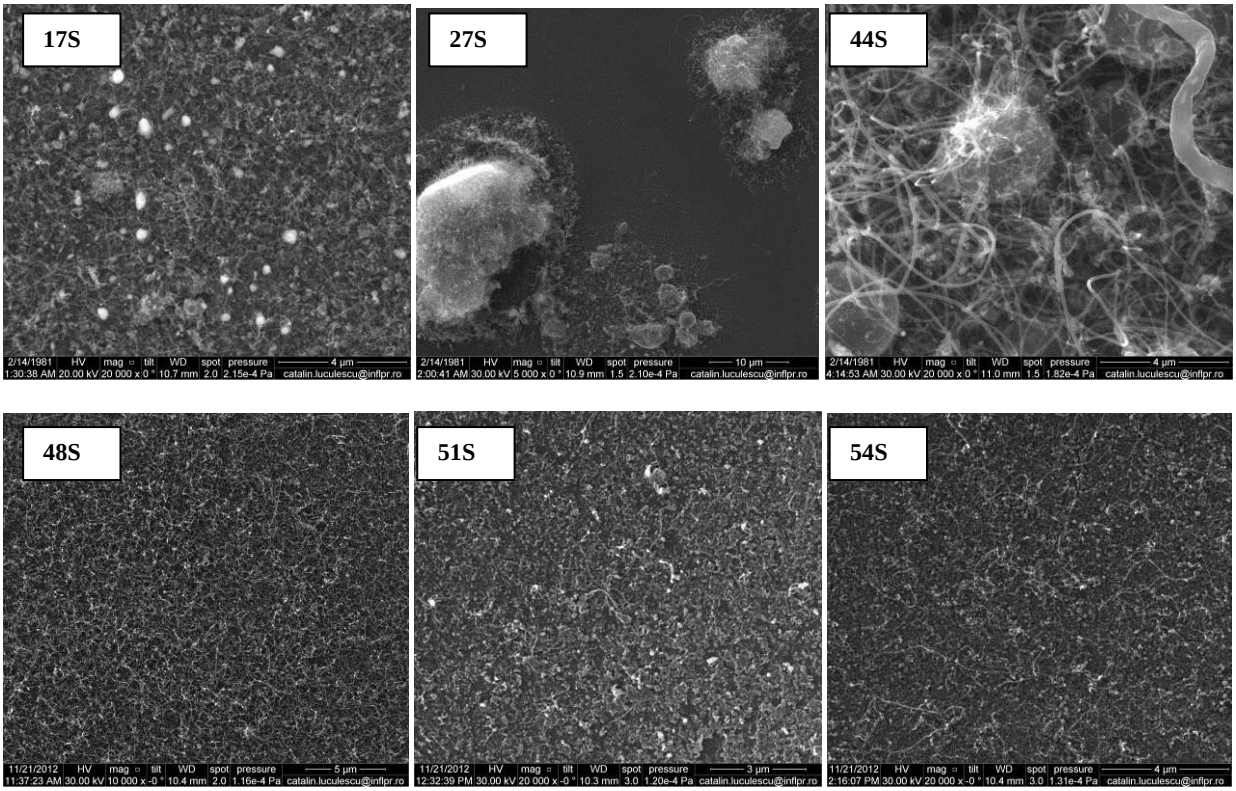

Fig. 3. SEM images of as CNT films growth by using concentrated catalytic suspension (samples 17S, 27S, 44S) and diluted catalytic suspension (samples 48S, 51S, 54S).

In Fig. 3, the upper SEM images represent samples obtained by using CCS. They reveal that most of Fe_2O_3 based nanoparticles catalyze the nucleation and growth of carbon nanotubes. As the ammonia concentration in the reactive mixture increases (samples 27S and 44S), the obtained CNT exhibit besides the fibrillose structures, large clusters of highly agglomerated nanotubes. These clumps are rare and randomly spread over the deposit surface. The origin of these large clusters was debated in the literature. It was hypothesized that the nanotubes/nanofibres are produced in clumps originating from the surface of the catalyst particles [15]. Another explanation for the formation of large agglomerates of CNTs concerns the tendency of the nanotubes to interact with each other due to surface forces. During their formation, CNTs have surface carboxyl groups and maybe some hydroxyl groups. These interact through hydrogen bonding or due to weak Van der Waals forces creating clusters and agglomerates [16]. On the contrary, the SEM images for the samples 51S and 54S obtained by using DCS, at the same laser power and C_2H_2/NH_3 ratio like samples 27S and 44S, reveal only few CNTs. The highest densities of CNTs were obtained for the samples 17S and 48S, that are synthesized at the lowest flow of NH_3 (90 sccm), and at a relatively low laser power (55 W), although different concentrations of catalyst solutions were involved.

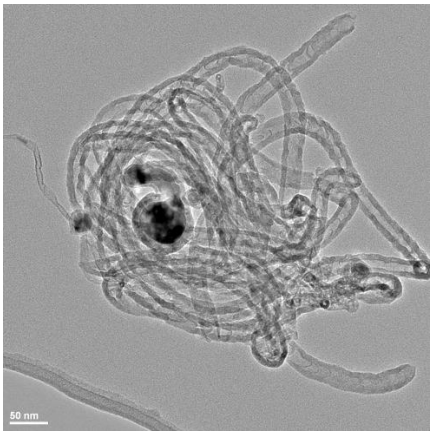

Fig. 4. Medium resolution TEM image of carbon nanotubes detected in sample 27S.

The TEM image of the sample 27S obtained with mean NH_3 concentration indicates the formation of multi-wall carbon nanotubes (MWCNT) with bamboo-like structure (Fig. 4). The formation of bamboo-like structure could be attributed to nitrogen incorporation in the graphitic network, which induces the curvature of the graphitic layer [17].

4. Discussion

Generally, the size of the metal particles determines the diameter of the deposited CNTs [18-20]. We started from Fe_2O_3 based nanoparticles with a relative small mean diameter (5 nm) attempting to obtain similar size for the metallic Fe nanoparticles after the NH_3 etching (reduction) step. Due to both the dominant role played by the surface energy for a nanoscale particle and to the high percentage of surface atoms in case of very small catalysts, the graphite deposes as curved shells on their surface, with their edges strongly chemisorbed to the metal [7]. Because the surface energy is inversely proportional to the surface area, small catalyst particles have a higher surface energy than the bigger ones. Consequently, the smaller particles will favour the CNTs growth.

Baker and Harris reported that that unsaturated hydrocarbons such as C_2H_2 had much higher yields and higher deposition rates than more saturated gases (e.g., C_2H_4) [21]. Ammonia plays the role of an energy transfer agent, due to the resonant absorption of the IR radiation. Indeed, the CO_2 laser serves as a local heat source, heating both the substrate and the gas phase. So, if ammonia is added in the reactant gases, the absorption of laser radiation is enhanced. However, acetylene decomposition at the interface should likely occur due to both the high temperatures reached by the irradiated substrate and to the partial contact with the hot iron- based particles (metal particles have a high thermal conductivity). One has to remember that the catalysts do not only serve as nucleation sites, but also they promote the pyrolysis of acetylene. It is also known, that the C_2H_2 decomposition ($C_2H_2 \leftrightarrow 2C+H_2$) is an exothermic process.

Due to small size of catalyst particles, heat transfer analysis [22] shows that thermal equilibrium between the substrate and the catalyst is rapidly established and the temperature of the metal particles is the same as the substrate. Thermal decomposition of hydrocarbon molecules into carbon radicals occurs when the substrate temperature exceeds the threshold pyrolysis temperature of the precursor gas. The carbon atoms resulted from these radicals dissolve and diffuse through the metal particles and are precipitated on its surface in the form of carbon tubes. The carbon diffusion parameter depends on the dimensions of the particles, the characteristics of the metal used as catalyst, the temperature and the reactant gases involved in the process.

5. Conclusions

By systematically investigating the effect of catalyst density on CNT growth, we draw the following conclusions:

1. For the same gas flows and laser powers, a higher catalysts density at the interface will increase their ability to absorb the laser radiation, thus leading simultaneously to the increased temperature of the support and to the decreased reflected radiation. This statement can be observed from the comparison between SEM images and can be also confirmed by the calculated I_D/I_G and $I_{G'}/I_G$ ratios, respectively.

2. It is important to underline the complexity of the CNTs growth by C-LCVD. As the NH_3 concentration increases, the absorption of the laser radiation is enhanced, leading to a decreased temperature at the support surface. Consequently, in order to obtain a better graphitization of the CNTs when there is an increase of NH_3 concentration, it is necessary to increase the laser power. Much more, for rather low laser powers and high NH_3 flows (50-55 W and 180-270 sccm respectively), the use of DSC as precursors is no more leading to CNT formation and growth.

Further studies concerning the decomposition of acetylene/ammonia-based precursor over suitable nanocatalysts seeded on a silicon substrate and the influence of nitrogen incorporation in the CNTs produced by C-LCVD are underway.

Acknowledgement

The first author (I. P. M.) gratefully acknowledges financial support in the frame of the Project POSDRU/89/1.5/S/63700.

References

[1] Carbon Nanotubes: Science and Applications, M. Meyyappan ed., CRC Press, Boca Raton, FL, USA (2004).
[2] R. Andrews, D. Jaques, A. M. Rao, F. Derbshire, D. Qian, X. Fan, E. C. Dickey, J. Chen, Chem. Phys. Let, **303,** 467 (1999).
[3] K. Bladh, L. K. L. Falk, F. Rohmund, Appl. Phys. A **70**, 317 (2000).
[4] S. Iijima, Nature **354**, 56 (1991).
[5] A. A. Puretzky, H. Schittenhelm, X. Fan, M. J. Lance, L. F. Allard Jr., D. Geohegan, Phys. Rev. B. **65**, 245425 (2002).
[6] A. Moisala, A. G. Nasibulin, E. I. Kauppinen, J. Phys.: Condens. Matter **15**, S3011 (2003).
[7] M. A. Signore, A. Rizzo, R. Rossi, E. Piscopiello, T. Di Luccio, L. Capodieci, T. Dikonimos, R. Giorgi, Diam. Relat. Mater. **17**, 1936 (2008).
[8] M. Gaillard, C. Boulmer-Leborgne, N. Semmar, E. Millon, A. Petit, Appl. Surf. Sci., **258**, 9237 (2012).
[9] O. A. Nerushev, R.-E. Morjan, E. E. B.Campbell, F. Rohmund, J. Appl. Phys., **93**, 4185 (2003).

[10] I. Morjan, R. Alexandrescu, I. Soare, F. Dumitrache, I. Sandu, I. Voicu, A. Crunteanu, E. Vasile, V. Ciupina, S. Martelli, Mate. Sci. & Eng. C, **23**, 211 (2003).
[11] I. Morjan, I. Soare, R. Alexandrescu, L. Gavrila-Florescu, R.-E. Morjan, G. Prodan, C. Fleaca, I. Sandu, I. Voicu, F. Dumitrache, E. Popovici, Infr. Phys. & Tech., **51**, 186 (2008).
[12] E. F. Antunes, A. O. Lobo, E. J. Corat, V. J. Trava-Airoldi, A. A. Martin, C. Verıssimo, Carbon **44**, 2202 (2006).
[13] S. Scalese, V. Scuderi, S. Bagiante, I. Deretzis, A. La Magna, C. Bongiorno, G. Compagnini, S. Gibilisco, N. Piluso, V. Privitera, J. Raman Spectrosc. **43**, 1018 (2012).
[14] R. A. DiLeo, B. J. Landi, R.P. Raffaelle, J. Appl. Phys, **101**, 064307 (2007).
[15] S. Ratkovic, E. Kiss, G. Boskovic, Chem Ind Chem Eng Q **15**, 263 (2009).
[16] D. Bikiaris, Materials **3**, 2884 (2010).
[17] J. W. Jang, C. E. Leea, S. C. Lyu, T. J. Lee, C. J. Lee, Appl Phys Lett **84**, 2877 (2004).
[18] Y. Li, W. Kim, Y. Zhang, M. Rolandi, D. Wang, H. Dai, J. Phys. Chem. B **105**, 11424 (2001).
[19] C. L. Cheung, A. Kurtz, H. Park, C. M. Lieber, J. Phys. Chem B **106**, 2429 (2002).
[20] Y. Li, J. Liu, Y. Wang, Z. L.Wang, Chem. Mater. **13**, 1008 (2001).
[21] R. T. K. Baker, P. S. Harris, in Chemistry and Physics of Carbon, edited by P. L. Walker, Jr. and P. A. Thrower, New York, 1978), p. 83.
[22] F. Incropera, D. Dewitt, Fundamentals of heat and mass transfer, 4th edition John Wiley and Sons, New York (1996).

*Corresponding author: iuliana.soare@inflpr.ro